

Electromagnetic effects on the light hadron spectrum

S Basak¹, A Bazavov², C Bernard³, C DeTar⁴, E Freeland⁵, J Foley⁴,
 Steven Gottlieb⁶, U M Heller⁷, J Komijani³, J Laiho⁸, L Levkova⁴,
 R Li⁶, J Osborn⁹, R L Sugar¹⁰, A Torok⁶, D Toussaint¹¹,
 R S Van de Water¹² and R Zhou¹² [MILC Collaboration]

¹ NISER, Bhubaneswar, Orissa 751005, India

² Department of Physics and Astronomy, University of Iowa, Iowa City, IA 52240, USA

³ Department of Physics, Washington University, St. Louis, MO 63130, USA

⁴ Department of Physics and Astronomy, University of Utah, Salt Lake City, UT 84112, USA

⁵ Liberal Arts Department, School of the Art Institute of Chicago, Chicago, IL, USA

⁶ Department of Physics, Indiana University, Bloomington, IN 47405, USA

⁷ American Physical Society, One Research Road, Ridge, NY 11961, USA

⁸ Department of Physics, Syracuse University, Syracuse, NY 13244, USA

⁹ ALCF, Argonne National Laboratory, Argonne, IL 60439, USA

¹⁰ Physics Department, University of California, Santa Barbara, CA 93106, USA

¹¹ Physics Department, University of Arizona, Tucson, AZ 85721, USA

¹² Theoretical Physics Department, Fermilab, Batavia, IL 60510, USA

E-mail: sg@indiana.edu

Abstract. For some time, the MILC Collaboration has been studying electromagnetic effects on light mesons. These calculations use fully dynamical QCD, but only quenched photons, which suffices to NLO in χ PT. That is, the sea quarks are electrically neutral, while the valence quarks carry charge. For the photons we use the non-compact formalism. We have new results with lattice spacing as small as 0.045 fm and a large range of volumes. We consider how well chiral perturbation theory describes these results and the implications for light quark masses.

1. Introduction

The MILC collaboration has been studying electromagnetic and isospin-violating effects in pions and kaons for a number of years [1–4]. These effects are crucial for determining the three light-quark masses. The u , d , and s quark masses are both fundamental parameters of the standard model of elementary particle physics and important for phenomenology. The uncertainty in the size of the electromagnetic contributions to the pion and kaon masses is a major part of the error on each of the masses and the greatest source of error on the m_u/m_d mass ratio [5].

The electromagnetic error in m_u/m_d depends on the error in our estimate of $(M_{K^+}^2 - M_{K^0}^2)^\gamma$ where γ indicates the electromagnetic contribution to the difference in the squares of the charged and neutral kaon masses. (There is also a difference coming from the quark masses.) In 1960, Dashen [6] showed that at leading order electromagnetic mass splittings for the mesons are mass independent, *i.e.*, $(M_{K^+}^2 - M_{K^0}^2)^\gamma = (M_{\pi^+}^2 - M_{\pi^0}^2)^\gamma$. We can parameterize the higher order effects via a parameter ϵ defined by $(M_{K^+}^2 - M_{K^0}^2)^\gamma = (1 + \epsilon)(M_{\pi^+}^2 - M_{\pi^0}^2)^\gamma$. This definition of ϵ , which uses the experimental mass difference on the RHS, is slightly different from what we have used before, in which $(M_{\pi^+}^2 - M_{\pi^0}^2)^\gamma$ appears on the RHS.

Table 1. Parameters of the (2+1)-flavor asqtad ensembles used in this study. Volumes marked with * are currently used in the finite volume studies, but not in the full analysis. The quark masses m'_l and m'_s are the light and strange dynamical masses used in the runs. The number of configurations listed as ‘132+52’ for the $a \approx 0.12$ fm, $48^3 \times 64$ ensemble gives values for two independent streams, the first in single precision, and the second in double. At the moment, we treat them as separate data, and do not average the results.

$\approx a[\text{fm}]$	Volume	β	m'_l/m'_s	# configs.	L (fm)	$m_\pi L$
0.12	$12^3 \times 64^*$	6.76	0.01/0.05	1000	1.4	2.7
	$16^3 \times 64^*$	6.76	0.01/0.05	1303	1.8	3.6
	$20^3 \times 64$	6.76	0.01/0.05	2254	2.3	4.5
	$28^3 \times 64$	6.76	0.01/0.05	274	3.2	6.3
	$40^3 \times 64^*$	6.76	0.01/0.05	115	4.6	9.0
	$48^3 \times 64^*$	6.76	0.01/0.05	132+52	5.4	10.8
	$20^3 \times 64$	6.76	0.007/0.05	1261	2.3	3.8
	$24^3 \times 64$	6.76	0.005/0.05	2099	2.7	3.8
0.09	$28^3 \times 96$	7.09	0.0062/0.031	1930	2.3	4.1
	$40^3 \times 96$	7.08	0.0031/0.031	1015	3.3	4.2
0.06	$48^3 \times 144$	7.47	0.0036/0.018	670	2.8	4.5
	$56^3 \times 144$	7.465	0.0025/0.018	433	3.3	4.4
	$64^3 \times 144$	7.46	0.0018/0.018	826	3.7	4.3
0.045	$64^3 \times 192$	7.46	0.0028/0.014	861	2.8	4.6

Our calculation is done with dynamical QCD but with quenched, noncompact QED. The analysis of Bijnens and Danielsson [7] shows that quenched QED is sufficient for a controlled calculation of ϵ at NLO in $SU(3)$ chiral perturbation theory.

In table 1, we list the ensembles of gauge configurations used for the results reported here. The two larger volume $a \approx 0.06$ fm and the $a \approx 0.045$ fm ensembles were not included in our results presented at Lattice 2014 [8]. The $40^3 \times 64$ and $48^3 \times 64$ ensembles with $\beta = 6.76$ were generated after Lattice 2014 and first discussed at this conference, but they are included in Ref. [8].

2. Finite volume effects

Because the photon is massless, finite volume effects are an important issue and a source of uncertainty in our earlier results. For $a \approx 0.12$ fm, we had volumes of $20^3 \times 64$ and $28^3 \times 64$ and found small finite volume effects compared to what was seen in Ref. [9]. Electromagnetic finite volume effects have been calculated by Hayakawa and Uno [10] using chiral perturbation theory. They found rather large effects; however, there is not a unique choice of how to treat finite-volume zero modes for the $U(1)$ field in the noncompact formalism. For the temporal modes A_0 in Coulomb gauge, all modes for 3-momentum $\vec{k} = 0$ must be dropped. That is, $A_0(\vec{0}, k_0) = 0$ for all k_0 . For the spatial modes, the action density is $[(\partial_0 A_i)^2 + (\partial_j A_i)^2]/2$, so the only mode that must be dropped is that with $(\vec{k}, k_0) = (\vec{0}, 0)$. Hayakawa and Uno dropped all A_i modes with $\vec{k} = 0$. However, we have only dropped modes with both $\vec{k} = 0$ and $k_0 = 0$. In our case, the finite size effects are smaller, although the magnitude of the effect does depend on T/L where T (L) is the temporal (spatial) extent of the lattice. Figure 1 compares the finite volume effects for the two choices.

In order to test the prediction, we added four new volumes this year with $L = 12, 16, 40$, and 48. In Fig. 2, we show our results for six values of L . We plot electromagnetic splittings of squared masses $\Delta M_{xy}^2 \equiv M_{xy}^2 - M_{x'y'}^2$, where the first meson is constructed from valence quarks

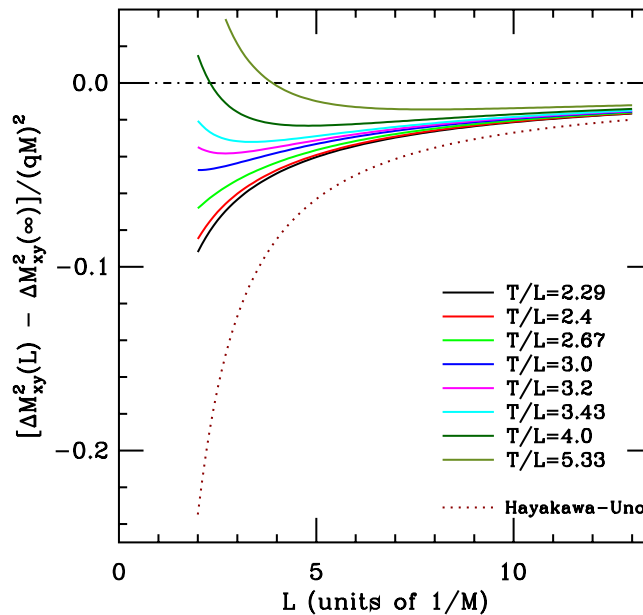


Figure 1. Comparison of electromagnetic finite volume (FV) effects in our scheme with that in Ref. [10]. q and M are the charge and mass of the meson, respectively. The values of T/L correspond to aspect ratios used in our ensembles, with 4.0 and 5.33 corresponding to the two smallest volumes in our FV study. Our FV effects are a factor of 2–3 smaller in most of the relevant range.

x and y with charges q_x, q_y and masses m_x, m_y , and the second meson is made from quarks x' and y' with the same masses but with the quark charges set to zero. To compare results from different ensembles, we multiply the squared-mass difference by r_1^2 where r_1 is a length scale determined from the static potential. Each curve is a fit with a single parameter, the infinite volume limit. In other words, the shape of the curve, but not its height, is determined by the theory. The horizontal lines show the infinite volume limit for two mass combinations labeled ‘pion’ and ‘kaon.’ It is now clear why we saw such a small difference between $L = 20$ and 28. The slope of each curve is low in that region. It is also worth noting that for the ‘pion,’ the sign of the effect changes within the range of our new calculation. With our improved understanding of the finite volume effects, we can more accurately adjust our results to the infinite volume limit with a smaller residual error. This reduces our errors on ϵ and m_u/m_d , as we show later.

3. Chiral fit and extrapolation

We have calculated meson masses for a large number of valence-quark mass and charge combinations. On some ensembles, we include charges larger than the physical values. On others, we calculated all combinations of charges $\pm 2/3e$, $\pm 1/3e$, and 0. In the first step of the analysis, values are corrected for finite-volume effects. The corrections are 7–10% for pions (mesons with two light quarks) and 10–18% for kaons (mesons with one light quark and one whose mass is near the strange quark mass). Because of the high level of correlation among the many meson masses, we thin the data set and sometimes have to consider uncorrelated fits. A typical fit might include 150 points.

Once the chiral fit for uncharged sea quarks is determined, we can set valence and sea quark masses equal, set m_s to its correct value and take the continuum limit. We then set the sea quark charges to their physical value using the NLO chiral logs. The last adjustment is very small for the kaon and vanishes identically for the pion. Figure 3 shows a small subset of the data for the uncorrelated fit that determines our central value. Note how much smaller the electromagnetic effects are for the neutral mesons (right).

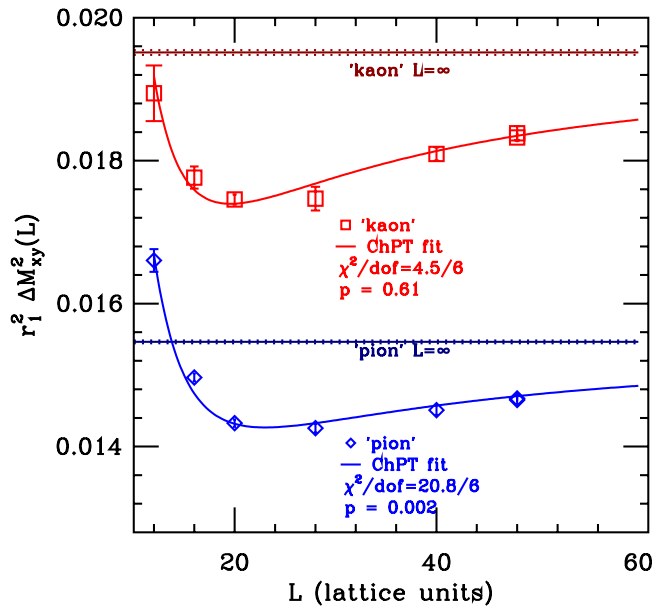


Figure 2. Finite volume effects at $a \approx 0.12$ fm and $am'_l = 0.01$, $am'_s = 0.05$ as a function of spatial lattice length L for two different meson masses: a unitary ‘pion’ (blue) with degenerate valence masses $m_x = m_y = m'_l$, and a ‘kaon’ (red) with valence masses $m_x = m'_l$ and $am'_y = 0.04$, close to the physical strange quark mass. The fit lines are to the FV form from SXPT, and have one free parameter each, the infinite volume value (shown by horizontal solid lines with dotted lines for errors).

There is a complication involving the neutral pion. The physical pion propagator involves disconnected diagrams in which the quark and anti-quark annihilate. These contributions are difficult to calculate accurately because they are noisy. We drop the disconnected diagrams and use the RMS average mass of $u\bar{u}$ and $d\bar{d}$ mesons. We denote this state as “ π^0 .” However, electromagnetic contributions to neutral mesons vanish in the chiral limit, so both the true $(M_{\pi^0}^2)^\gamma$ and our $(M_{\pi^0}^2)^\gamma$ are small.

In the last stage of the analysis, we subtract our results for the “ π^0 ” and K^0 from the corresponding charged meson to arrive at the physical electromagnetic mass differences. This is shown as the purple lines on the LHS of Fig. 3. The vertical lines represent the appropriate sum of quark masses for the charge-averaged pion and kaon masses. The horizontal line is the experimental value of the pion splitting. Thus, the distance between the horizontal line and the intersection of the purple line with the vertical, dashed-dotted physical pion line is an indication of the size of the systematic error. Looking at the ratio of the experimental result for the pion splitting to our kaon splitting, we get $\epsilon = 1.02(4)$. Alternatively, we may use our result for the electromagnetic pion splitting, and we find $\epsilon = 0.84(5)$. We have recently added the newer ensembles with $a \approx 0.06$ and 0.045 fm to our analysis. In this case, we drop the $a \approx 0.12$ fm ensembles and can get good correlated fits when the data is thinned. One such fit is shown in Fig. 4. In this case, we see that our result for the pion splitting is a bit low. This results in $\epsilon = 0.97(5)$. If we take the experimental value of the pion splitting, our result is $\epsilon = 0.83(4)$.

4. Results and future plans

Our current (preliminary) result for ϵ does not include the fit shown in Fig. 4, but it does include other variations on the fits shown in Fig. 3 in which different subsets of our data are included. Our result is [8]

$$\epsilon = 0.84(5)_{\text{stat}}(18)_{a^2}(6)_{\text{FV}} . \quad (1)$$

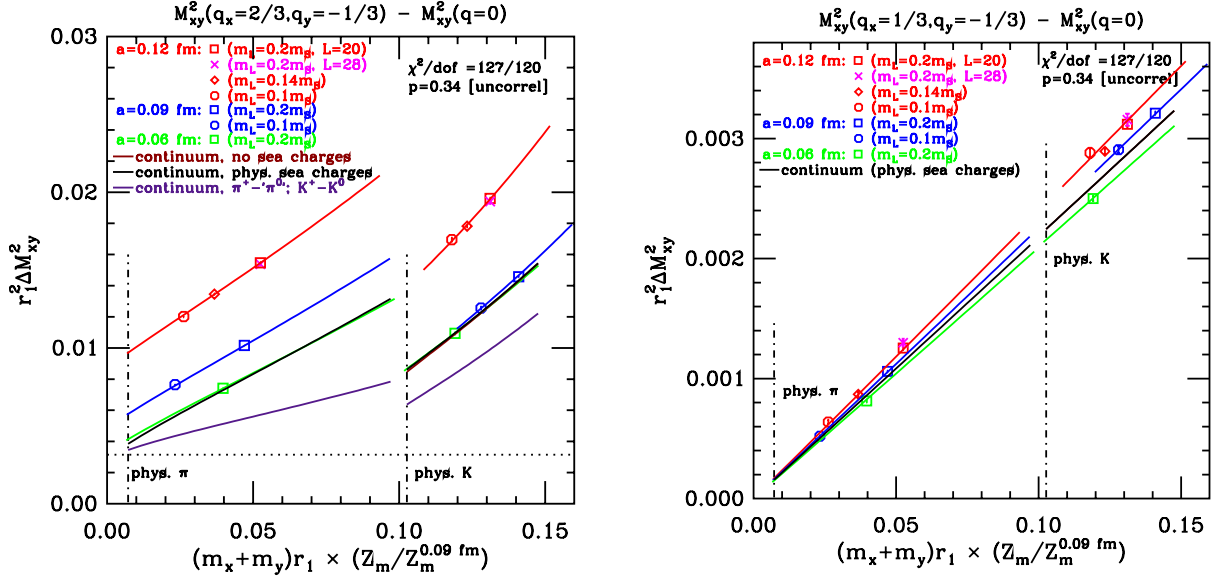


Figure 3. Central fit to the EM splitting ΔM_{xy}^2 vs. the sum of the valence-quark masses. Only a small subset of the partially quenched data set included in the fit is shown: the points for $a \approx 0.09$ fm and ≈ 0.06 fm, as well as the ‘pion’ (x -axis value < 0.07) points for $a \approx 0.12$ fm, have unitary values of the valence masses, while the ‘kaon’ (x -axis value > 0.1) points for $a \approx 0.12$ fm have $m_x = m_l'$ but $m_y = 0.8m_s'$, which is closer to the physical strange mass than m_s' itself. The data have been corrected for finite volume effects using NLO SXPT. The red, blue, and green curves correspond to the three lattice spacings. The black and purple curves are extrapolations, see text.

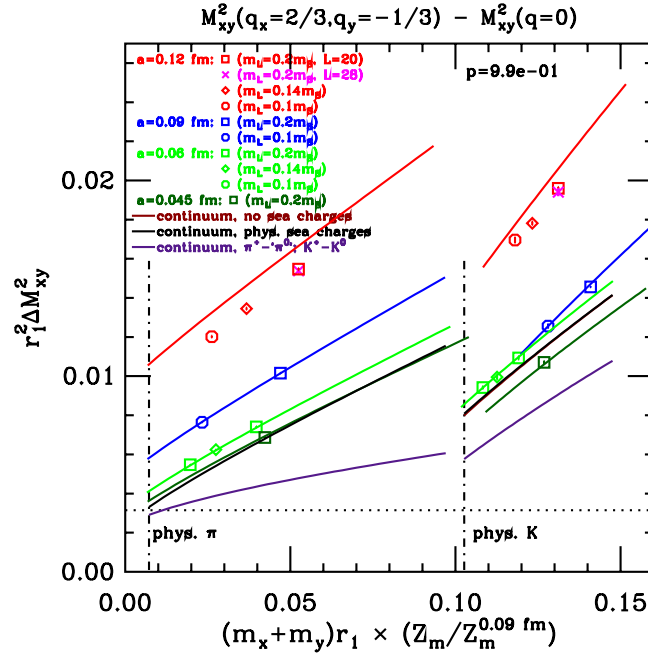


Figure 4. Similar to Fig. 3 except that $a \approx 0.12$ fm ensembles are not included in the fit and the correlations are included. Only a subset of the fitted data is shown.

The first error is statistical, the second from variations in the continuum extrapolation, and the third is our (hopefully conservative) estimate of the residual finite volume error that may remain after our correction based on the NLO formula. Previously, we have determined m_u/m_d by using our pseudoscalar mass results on our asqtad ensembles. However, we have recently been generating highly improved staggered quark (HISQ) ensembles for which the chiral extrapolation is much better controlled. Using our new value of ϵ in Eq. (1) with the HISQ light meson masses [11] gives a preliminary value for the ratio

$$m_u/m_d = 0.4482(48)_{\text{stat}} \left(\begin{smallmatrix} +21 \\ -115 \end{smallmatrix} \right)_{a^2} (1)_{\text{FV}_{\text{QCD}}} (165)_{\text{EM}}, \quad (2)$$

where here “EM” denotes all errors from electromagnetism, while “FV_{QCD}” refers to finite-volume effects in the pure QCD calculation. The electromagnetic error has been reduced by more than a factor of two from our previous result [5].

We plan on several future improvements. First, we will continue to analyze the ensembles that were not in our prior work. We will also repeat the analysis of quenched electromagnetic effects on the HISQ ensembles. The HISQ ensembles have several advantages. They should have smaller discretization errors, and the chiral extrapolation errors should be much smaller, as we have ensembles tuned to the physical light quark mass. Finally, the finite volume errors should be reduced as the HISQ lattices are larger than those for asqtad. We are also working on a fully dynamical $SU(3) \times U(1)$ code to allow us to include charged sea-quark mass effects [12]. This will make possible controlled calculations of many additional quantities. We have also calculated electromagnetic effects on the baryon spectrum, but did not have time to report on that.

Acknowledgments

The spectrum running was done on computers at the National Center for Supercomputing Applications, Indiana University, the Texas Advanced Computing Center (TACC), and the National Institute for Computational Science (NICS). Configurations were generated with resources provided by the USQCD Collaboration, the Argonne Leadership Computing Facility, and the National Energy Research Scientific Computing Center, which are funded by the Office of Science of the U.S. Department of Energy; and with resources provided by the National Center for Atmospheric Research, NICS, the Pittsburgh Supercomputer Center, the San Diego Supercomputer Center, and TACC, which are funded through the National Science Foundation’s XSEDE Program. This work was supported in part by the U.S. DOE and the NSF.

References

- [1] Basak S *et al.* (MILC Collaboration) 2008 *PoS LATTICE2008* 127 (*Preprint* 0812.4486)
- [2] Torok A, Basak S, Bazavov A, Bernard C, DeTar C *et al.* 2010 *PoS LATTICE2010* 127
- [3] Basak S *et al.* (MILC Collaboration) 2012 *PoS LATTICE2012* 137 (*Preprint* 1210.8157)
- [4] Basak S *et al.* (MILC) 2013 *PoS CD12* 030 (*Preprint* 1301.7137)
- [5] Bazavov A, Toussaint D, Bernard C, Laiho J, DeTar C *et al.* 2010 *Rev.Mod.Phys.* **82** 1349–1417 (*Preprint* 0903.3598)
- [6] Dashen R F 1969 *Phys.Rev.* **183** 1245–1260
- [7] Bijnens J and Danielsson N 2007 *Phys.Rev.* **D75** 014505 (*Preprint* hep-lat/0610127)
- [8] Basak S *et al.* (MILC Collaboration) 2014 *PoS LATTICE2014* (*Preprint* 1409.7139)
- [9] Portelli A, Durr S, Fodor Z, Frison J, Hoelbling C *et al.* 2011 *PoS LATTICE2011* 136 (*Preprint* 1201.2787)
- [10] Hayakawa M and Uno S 2008 *Prog.Theor.Phys.* **120** 413–441 (*Preprint* 0804.2044)

- [11] Bazavov A *et al.* (Fermilab Lattice, MILC) 2014 *Phys.Rev.* **D90** 074509 (*Preprint* 1407.3772)
- [12] Zhou R and Gottlieb S 2014 *PoS LATTICE2014* 024 (*Preprint* 1411.4115)